

MoM-based Path Loss Modelling in Rural Areas

Temwani J. Phiri, David B. Davidson, *Fellow, IEEE* and P. Gideon Wiid, *Member, IEEE*

Abstract—Path loss is an important parameter for coverage mapping and spectrum management. Of special interest in this study is the modelling of path loss at low antenna heights (under 10 m) and short ranges (less than 1 km). This is of relevance to site evaluation of advanced radio telescopes such as MeerKAT in respect of computing RFI threshold levels and investigating coupling mechanisms. Previously, RFI thresholds have been based on free space loss predictions and are therefore inaccurate. We present a full-wave propagation model (FWPM) for path loss modelling in rural areas. Electrical characteristics of the earth are included and full antennas are modelled in order to reproduce a real world scenario. Statistical error analysis of the predictions yields an unprecedented RMSE of less than 4 dB when compared to measurements obtained at the MeerKAT facility.

I. INTRODUCTION

PROPAGATION modelling is an important tool in the rollout of a radio link with respect to assessing interference effects in the intervening path. The goal is to quantify the degree of signal degradation between wireless transceivers due to reflection, diffraction, scattering and other propagation phenomena besides spreading (free space) loss. Expressed as the ratio of transmitted to received power, the extent of signal attenuation is called *path loss*. It is a vital parameter for coverage mapping and spectrum management [1], [2]. Numerous path loss prediction tools utilizing theoretical, statistical, empirical and deterministic schemes have been developed over the last seven decades [3], [4]. This highlights the significance of propagation modelling in planning various types of wireless networks. Empirical models (synthesized based on multiple measurements) tend to be most common due to their ease of implementation. However, the predictions quickly become inaccurate when they are employed in an environment other than the one on which the data is based. On the other end of the spectrum, deterministic models (derived from Maxwell's equations) offer high accuracy but require detailed information of the environment (site-specific) and are computationally expensive [4], [5].

Unsurprisingly, the vast majority of models focus on mobile radio services in urban areas as well as FM radio and television broadcast services. In the former case, propagation is typically by diffraction and scattering since there are seldom line of sight (LoS) paths. Consequently, a multipath environment exists since the received signal is a superposition of several delayed waves [6]. In this regime, multipath fading – the variability of the wave due to constructive and destructive interference – becomes particularly important and is accounted for using a Rayleigh probability distribution [7]. In the latter scenario, atmospheric scattering and refraction are the

characteristic propagation effects. The physical configuration involves transmitting (base) stations that are hundreds of metres high with a coverage radius extending a few tens of kilometres. One thus finds that models addressing propagation in open areas are few and far between and do not typically consider short transmitter-receiver (T-R) separation distances. With the outset of advanced and highly sensitive radio telescopes such as the Square Kilometre Array (SKA), probing signal propagation at path lengths and heights that differ from conventional telecommunication standards becomes important. Moreover, literature is thin on propagation modelling to aid electromagnetic characterization of radio astronomy facilities. We thus present a novel full-wave propagation model (FWPM) based on the method of moments (MoM) for path loss predictions at T-R lengths less than 1 km. Electrical properties of the earth are taken into account and simulated as a dielectric ground plane. Combined with the full-wave nature of the model, the ground-reflected wave is thus approximated very well. In its present form, the FWPM has no restriction on frequency but is presently limited to the range 100 – 2700 MHz which falls within the mid-frequency band of the SKA. As a case study, comparisons of the FWPM predictions are made to measured data obtained at the MeerKAT facility in South Africa's semi-desert Karoo region. Statistical error analysis yields an unprecedented 3.08 and 3.57 dB root mean square error for the two configurations considered.

The paper is fashioned with an overview on propagation modelling in Section II which introduces the statistical metrics used in the study. In Section III a description of the FWPM is provided and validated by a comparison to the Friis transmission equation. The main contributions are highlighted in Section IV where statistical analysis is made against measured data. Concluding remarks are presented in Section V.

II. OVERVIEW OF PROPAGATION MODELLING

A. Basic Modelling

In the log domain, a radio link is modelled as

$$P_r = \text{EIRP} + G_r - PL, \quad (1)$$

where P_r is the received power in dBm, $\text{EIRP} = P_t + G_t$ is the effective isotropic radiated power (dBm), G_t and G_r are the respective transmitter and receiver gains in dBi. The term PL (dB) is the attenuation (path loss) due to environmental and propagation effects given as

$$PL = L_{\text{fsl}} + L_{\text{env}}, \quad (2)$$

where L_{fsl} is the free space loss derived from the Friis transmission formula with isotropic transceivers as the reference. The term L_{env} is the loss due to reflection, diffraction or scattering depending on the propagation mode and surrounding

The authors are with the Department of Electrical and Electronic Engineering, Stellenbosch University, Stellenbosch 7600, South Africa (email: temwanijoshua@outlook.com; davidson@sun.ac.za; wiidg@sun.ac.za)

medium¹. In cases where a LoS path exists and the antennas are several wavelengths above the ground, equation (2) can be approximated as

$$PL = L_{\text{fsl}} = 10 \log \left[\left(\frac{4\pi d_m f}{c} \right)^2 \right], \quad (3)$$

where f (Hz) is the carrier frequency, d_m (m) is the T-R length and c (m/s) the speed of light in a vacuum. In practical units, equation (3) is given as

$$L_{\text{fsl}} = 20 \log(f) + 20 \log(d) + 32.45, \quad (4)$$

with f in MHz and $d = 10^{-3} d_m$ in km.

Propagation models strive to predict as accurately as possible the loss L_{env} . The general input parameters include frequency, antenna heights and T-R separation. More complex models such as the Longley-Rice Irregular Terrain Model (ITM) and the ITU-R P.452 model can incorporate terrain data in order to account for diffraction loss due to obstructions. Effectiveness of a model in predicting path attenuation depends on its input parameters as well as whether the model is applied within its coverage range. A wide survey of various models and how they predict PL is presented in [3].

B. Statistical Analysis Metrics

1) *Prediction Error and Root Mean Square Error*: The prediction error, ε , is the most basic of metrics in evaluating a propagation model. It is the difference between the measured and predicted value of path loss, given for a specific path as

$$\varepsilon_{m,i} = PL_{\text{meas}} - PL_{m,i}, \quad i = 1, 2, \dots, N \quad (5)$$

where subscript m denotes a model and N is the number of sample (frequency) points. The mean prediction error is simply

$$\bar{\varepsilon}_m = \frac{1}{N} \sum_{i=1}^N \varepsilon_{m,i}, \quad (6)$$

and its associated standard deviation is

$$\sigma_{\varepsilon_m} = \sqrt{\frac{\sum_{i=1}^N (\varepsilon_{m,i} - \bar{\varepsilon}_m)^2}{N-1}}. \quad (7)$$

A more qualitative description of a models performance is the root mean square error (RMSE)

$$\text{RMSE} = \sqrt{\frac{1}{N} \sum_{i=1}^N \varepsilon_{m,i}^2}, \quad (\text{dB}) \quad (8)$$

which is a measure of deviation from the measured value. Hence the RMSE serves as the standard error of the predictions.

¹Small-scale fading effects are neglected here

2) *Relative Error and Accuracy*: Relative Error (RE) is the magnitude of the prediction error weighted by the measured (true) value of path loss. It is the fractional error

$$\text{RE}_m = \frac{1}{N} \sum_{i=1}^N \frac{|\varepsilon_{m,i}|}{PL_{\text{meas}}}, \quad (9)$$

from which the accuracy $A_m = (1 - \text{RE}_m) \times 100$, can be calculated. The accuracy provides a confidence level for a models prediction.

3) *Correlation Coefficient*: Linear closeness between measurement and predictions is determined by the correlation coefficient

$$\rho = \frac{N \sum_{i=1}^N PL_{\text{meas}} PL_{m,i} - \sum_{i=1}^N PL_{\text{meas}} \sum_{i=1}^N PL_{m,i}}{(N-1) \sum_{i=1}^N PL_{\text{meas}} \sum_{i=1}^N PL_{m,i}}. \quad (10)$$

It must be noted here that strong correlation will not necessarily mean that a model performs well but rather indicates that the model exhibits similar trends as the measured data.

III. THE FULL-WAVE PROPAGATION MODEL

Numerical solutions to Maxwell's equations that make no *a priori* physical approximations are called full-wave techniques [8]. Computational electromagnetics (CEM) offers a number of such methods which are described in several texts (see [8]–[10]). The full-wave propagation model (FWPM) described here is based on the method of moments (MoM) implemented via the FEKO software suite. Other full-wave implementations are described in [18]–[20].

A. The Method of Moments

The MoM is a frequency domain full-wave technique widely used in antenna engineering as it is well suited to problems involving radiation and scattering. The method utilizes an appropriate Green function to derive an integro-differential form of Maxwell's equations. To reduce the number of unknowns and make the problem tractable computationally, a suitable boundary condition and *basis functions* must be selected. This results in a system of linear equations of the form [9],

$$V_m = \sum_{n=1}^{N-1} Z_{mn} I_n, \quad m = 1, 2, \dots, N-1 \quad (11)$$

where Z_{mn} is called the system matrix, V_m is the source vector and I_n is the unknown vector that is solved for using LU-factorization. Subscript m represents sampling points while n refers to source points. The MoM implementation in the FEKO software suite includes extensions that enable the modelling of dielectrics. Of special interest here is the Sommerfeld formulation and reflection coefficient approximation that are used to simulate 'real ground'.

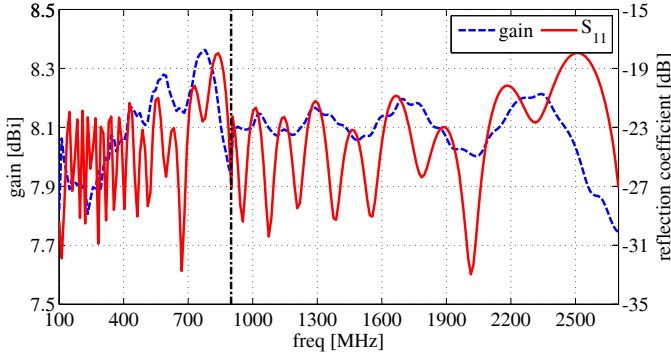


Fig. 1. Gain (dBi) and reflection coefficient (S_{11} , dB) of the LPDA's used for the FWPM simulations. The vertical dash-dot line corresponds to 900 MHz and demarcates the transition from band 1 to band 2.

B. Antenna Characteristics

The quality of radiation source data is a vital part of the FWPM. The initial intention had been to generate the data using half-wave dipoles but mismatch effects were too significant over the desired frequency range. In keeping with a relatively simple design, log-periodic dipole array (LPDA) antennas were realized in Antenna Magus and subsequently exported to FEKO. A bandwidth of 160% was achieved with centre frequencies of 500 MHz for band 1 (100 - 900 MHz) and 1500 MHz for band 2 (900 - 2700 MHz). Parametrized by a spacing factor of 0.131, 27 elements were used for each antenna. Load and input impedances were 292.19Ω and 200Ω , respectively. Fig 1 shows the gain and reflection coefficient of the antennas.

C. Influence of the Ground

Radio wave transmission that takes place in the vicinity of the earth is called ground wave propagation. Three waves are to be considered in general: surface, direct and ground-reflected waves. In many scenarios the contribution of the surface wave is negligible so that the received wave is predominantly the sum of the direct and ground-reflected waves, collectively called the space wave. In view of reflections, the electrical characteristics of the ground must be taken into account.

1) *Complex Permittivity*: Given a dielectric medium of permittivity ϵ^2 and effective conductivity σ , the Maxwell-Ampere equation can be written as [11]

$$\nabla \times \mathbf{H} = j\omega\epsilon\mathbf{E} + \sigma\mathbf{E} = j\omega \left[\epsilon - j\frac{\sigma}{\omega} \right] \mathbf{E} = j\omega\dot{\epsilon}\mathbf{E}, \quad (12)$$

where $\dot{\epsilon}$ is the complex permittivity³ that typifies the behaviour of a partially conducting dielectric. The relative complex permittivity can then be defined as

$$\dot{\epsilon}_r = \frac{\dot{\epsilon}}{\epsilon_0} = \epsilon_r - j\frac{\sigma}{\omega\epsilon_0} = \epsilon_r - jx. \quad (13)$$

²Not to be confused with prediction error, ϵ

³Strictly speaking complex permittivity is presented as $\dot{\epsilon} = \epsilon' - j\epsilon''$ [12]. However, in practice the macroscopic effect of the alternating field conductivity, $\omega\epsilon''$, is indistinguishable from the effect of σ .

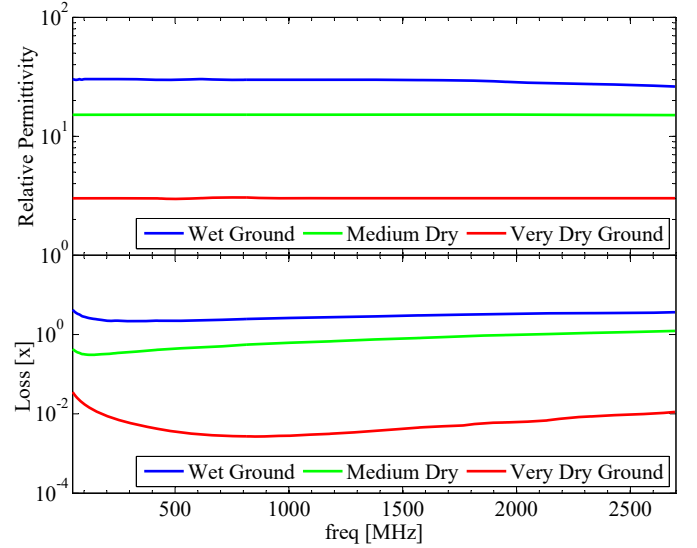


Fig. 2. Relative permittivity and the loss term x

Electrical characteristics of a given ground are summarized by $\dot{\epsilon}_r$. Relative permittivity and the loss term x are shown in Fig 2 for three types of ground as provided in [13].

2) *Plane Earth Reflection*: A simplified but practical approach to model ground wave propagation is [14], [15]

$$\frac{E}{E_0} = 1 + Re^{-j\Delta\phi} + (1 - R)Fe^{-\Delta\phi}, \quad (14)$$

where E and E_0 represent the received and free space electric fields, respectively. The term R represents the Fresnel reflection coefficients for vertical or horizontal polarization as shown in equations (16) and (17); F is the attenuation factor (equation (19)) that heavily influences the surface wave; the angle

$$\Delta\phi = \frac{\omega}{c} (R_2 - R_1) \quad (15)$$

accounts for the phase difference between the direct and reflected waves where

$$R_1 = d_m \sqrt{\left(\frac{h_t - h_r}{d_m} \right)^2 + 1}$$

and

$$R_2 = d_m \sqrt{\left(\frac{h_t + h_r}{d_m} \right)^2 + 1},$$

with d_m as the T-R length in metres as before. A schematic of the configuration is shown in Fig 3.

Reflection at the interface of two media is a well known and widely discussed phenomenon. For dielectrics, the reflection coefficient will be a function of the ratio of the permittivity of the two media, polarization and angle of incidence. It can be shown that setting the relative complex permittivity of the earth to $\dot{\epsilon}_r$ yields [11], [12]

$$R_v = \frac{\dot{\epsilon}_r \sin \psi - \sqrt{\dot{\epsilon}_r - \cos^2 \psi}}{\dot{\epsilon}_r \sin \psi + \sqrt{\dot{\epsilon}_r - \cos^2 \psi}}, \quad (16)$$

$$R_h = \frac{\sin \psi - \sqrt{\dot{\epsilon}_r - \cos^2 \psi}}{\sin \psi + \sqrt{\dot{\epsilon}_r - \cos^2 \psi}}, \quad (17)$$

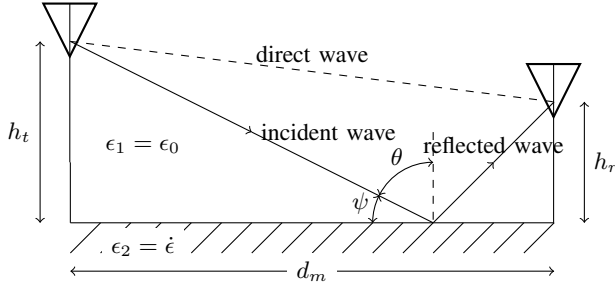


Fig. 3. Geometry of ground-reflected waves

as the the reflection coefficients for vertical (parallel) and horizontal (perpendicular) polarizations with

$$\psi = 90^\circ - \theta = \arctan\left(\frac{h_t + h_r}{d_m}\right) \quad (18)$$

as the angle of incidence (Fig 3). If the surface wave is required, the attenuation function is given by

$$F = \{1 - j\sqrt{\pi\nu}e^{-\nu} [\operatorname{erfc}(j\sqrt{\nu})]\}, \quad (19)$$

where erfc is the complementary error function. For vertical polarization, the term ν is given by

$$\nu_v = \frac{-j\omega d_m}{2\epsilon_r c} \left(1 - \frac{\cos^2 \psi}{\epsilon_r}\right) \left[1 + \frac{\epsilon_r \sin \psi}{\sqrt{\epsilon_r - \cos^2 \psi}}\right]^2, \quad (20)$$

while for horizontal polarization it is

$$\nu_h = \frac{-j\omega d_m}{2c/\epsilon_r} \left(1 - \frac{\cos^2 \psi}{\epsilon_r}\right) \left[1 + \frac{\epsilon_r^{-\frac{1}{2}} \sin \psi}{\sqrt{\epsilon_r - \cos^2 \psi}}\right]^2. \quad (21)$$

The FWPM results presented here make use of the reflection coefficient approximation which does not compute the surface wave. However, at the expense of longer simulation runtime the model can be set to utilize the full Sommerfeld formulation which will incorporate the contribution of the surface wave to the received field.

D. Simulation Setup and Validation

Simulated path loss was computed via S-Parameters as

$$PL_s = 10 \log \left| \frac{1}{S_{21}'} \right|^2 + 2G, \quad (22)$$

where $|S_{21}'|^2 \equiv$ power received/power radiated is the transmission coefficient corrected for mismatch and G is the gain of transmitter and receiver in dBi. To ensure that the FEKO model was correctly configured, a comparison was made to theory (equation (4)). As can be seen from the sample result in Fig 4, the simulated prediction is in good agreement with the theoretical formulation of the Friis transmission equation. This is quite a remarkable result that highlights the power of a full-wave simulation.

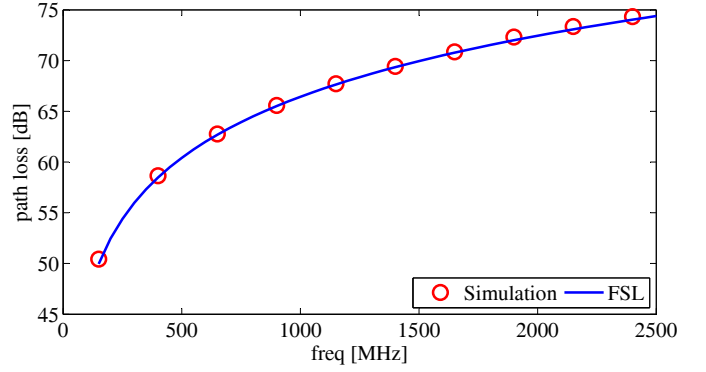


Fig. 4. Free space path loss predictions at a T-R distance of 50 m

TABLE I
EQUIPMENT USED FOR VERIFICATION MEASUREMENTS

| | |
|--------------------------------------|------------------|
| AnaPico APSIN6010 DC Generator | |
| output power (used) | -20 dBm |
| frequency range | 0.009 – 6100 MHz |
| PCB-LPDA (transmitter and receiver) | |
| average gain | 5 dBi |
| frequency range | 400 – 6000 MHz |
| FSH4 Handheld Spectrum Analyser (SA) | |
| sensitivity | -141 dBm |
| frequency range | 0.009 – 3600 MHz |

IV. COMPARISON OF FWPM PREDICTIONS TO MEASURED DATA

A. Measurements in a Controlled Environment

Path loss results can change quite dramatically when transmission takes place in the vicinity of the ground such as when transceiver heights are low. In a ‘simple’ scenario involving a flat ground, the key issue for the FWPM is with regard to the value of ϵ_r in modelling the electrical characteristics of the earth. Conditions of the soil change with seasonal variations so that the actual electrical parameters will seldom be known. A working approximation must thus be established. To do this, predictions from three types of simulated ground were compared to measured data that was obtained at a field akin to an open area test site. A summary of the equipment used is presented in Table I.

A PCB-LPDA was connected to the Anapico DC signal generator to form the transmitting unit while the receiver unit comprised a similar PCB-LPDA and the FSH4 handheld spectrum analyser. With the transmitting antenna fixed at a height of 5 m and the receiving antenna at 2 m, the maximum received power was recorded at five distances between 20 and 200 m. Some results are shown in Fig 5 while statistical analysis of the predictions is presented in Table II. Although all three FWPM simulations yield very good predictions, based on the root mean square errors the best approximation to the measurement scenario is the medium dry ground setup. More

TABLE II
MEAN PREDICTION ERROR AND RMSE ANALYSIS FOR THE FWPM VALIDATION

| d_m | Prediction Error, $\bar{\epsilon}$ [dB] | | | | Max Residual, ϵ_{\max} [dB] | | | | Standard Dev, $\sigma_{\bar{\epsilon}}$ [dB] | | | | RMSE [dB] | | | |
|-------|---|------|------|------|--------------------------------------|-------|-------|-------|--|------|------|------|-----------|------|------|------|
| [m] | dry | med | wet | FSL | dry | med | wet | FSL | dry | med | wet | FSL | dry | med | wet | FSL |
| 20 | 1.96 | 2.36 | 2.65 | 8.41 | 8.44 | 7.42 | 8.34 | 13.87 | 2.85 | 2.19 | 2.22 | 2.33 | 3.46 | 3.22 | 3.45 | 8.73 |
| 50 | 2.50 | 2.92 | 3.25 | 8.35 | 16.05 | 14.76 | 14.06 | 19.70 | 3.92 | 3.71 | 3.92 | 4.44 | 4.65 | 4.71 | 5.09 | 9.45 |
| 100 | 2.54 | 2.69 | 2.82 | 6.86 | 13.40 | 12.67 | 12.23 | 18.13 | 5.54 | 4.58 | 4.08 | 3.73 | 6.09 | 5.31 | 4.96 | 7.81 |
| 150 | 0.91 | 1.21 | 1.42 | 5.74 | 16.33 | 16.18 | 16.17 | 23.21 | 4.30 | 3.84 | 3.71 | 5.03 | 4.39 | 4.02 | 3.96 | 7.63 |
| 200 | 2.01 | 1.98 | 1.97 | 4.54 | 8.00 | 8.02 | 8.04 | 11.21 | 1.87 | 1.97 | 2.06 | 2.97 | 2.75 | 2.78 | 2.85 | 5.43 |
| mean | 1.99 | 2.23 | 2.42 | 6.78 | 12.44 | 11.81 | 11.77 | 17.22 | 3.70 | 3.26 | 3.20 | 3.70 | 4.27 | 4.01 | 4.06 | 7.81 |

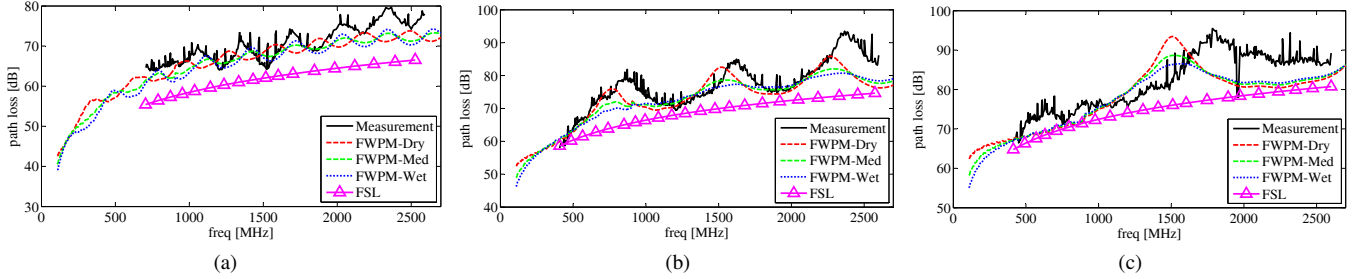


Fig. 5. Open area measurements and predicted path loss at T-R separations of (a) 20 m, (b) 50 m and (c) 100 m. In all cases $h_t = 5$ m and $h_r = 2$ m

significantly, it can be seen that the question of path loss below 1 km is not trivially equivalent to free space loss as often presumed. The maximum residual for FSL predictions lies 4.65 standard deviations from the mean but is 3.68 for the worst performing FWPM prediction. Evidently, free space path loss exhibits a significant deviation which can be costly where accuracy is required.

B. Case Study: Field Measurements in the Karoo

The Karoo is a semi-desert region in South Africa's Northern Cape Province and is home to MeerKAT – a Square Kilometre Array Telescope precursor. Propagation modelling has a vital role to play in the furtherance of good EMC and spectrum management practices wherein predictions form part of the basis on which RFI threshold levels are determined. The need for accuracy cannot therefore be overstated. Recently, a comparative study used data obtained at the MeerKAT site to examine the efficacy of ITU-R P.1546 and ITM models for path loss predictions at shorter path lengths and lower transceiver heights than originally intended [16]. While acceptable error margins were reported, it is desirable to achieve higher accuracy and synthesize a site-specific model to aid electromagnetic characterisation of the MeerKAT environment.

Karoo data analysed here is the same dataset as in [16]. Equipment used during the measurement campaign included a CPS1 pulse generator, LPDA (R&S HL033) and a horn antenna (EM-7020) at the transmitting end. On the receiving end, two LPDA's (R&S HL023 and a custom-built PCB-LPDA) were deployed in conjunction with a real-time analyser (RTA). Use of the pulser and RTA made broadband time-domain recordings possible, speeding up the survey time

significantly. Measurements were recorded for vertical polarization transmissions at five T-R separation distances between 50 and 3600 m for transmitter heights of 5 and 7.5 m. With free space loss as a reference, measured and predicted path loss curves are shown in Figs 6 and 7.

Statistical analysis on the FWPM predictions is provided in Table III. The row designated mean 1 is the average value corresponding to path lengths below 1 km while mean 2 is the average across all path lengths. Predictions of the free space loss (FSL) model are acceptable in respect of the 10 – 15 dB RMSE allowance for rural areas. Under a kilometre, 6.70 and 8.06 dB were obtained for the two respective cases, while 11.22 and 11.53 dB were obtained overall. However, if the individual path is considered, FSL predictions fall outside the acceptable margin above 1 km. In contrast, 3.08 and 3.57 dB RMSE is obtained overall for the FWPM predictions.

In terms of relative error, the FWPM yields a fractional error that is less than 0.05 which is equivalent to a confidence level (accuracy) greater than 95 % which is desired. FSL modelling fails this test with 93 % accuracy at best. Correlation is strong for both models particularly at short ranges. Slightly more linear closeness is seen in the FSL model in the second configuration ($h_t = 7.5$ m) but overall the FWPM performs better with correlation coefficients of 0.729 and 0.795 versus 0.633 and 0.757 for FSL.

Electrical parameters corresponding to wet ground were found to provide the best fit to Karoo data. Assuming that the predominant source of attenuation is ground loss, this would suggest that the relative permittivity of Karoo soil is on the order of 32. This value stands in stark contrast to attempts that have been made at extracting the complex permittivity of Karoo soil such as in [17] where a value of 3.8 (typical for dry ground) is reported for the S and X bands. However, this

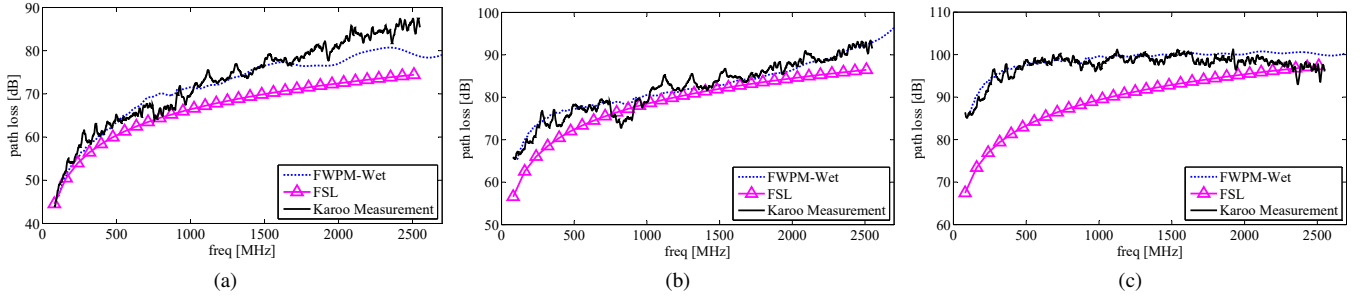


Fig. 6. Measured and predicted path loss in the Karoo: $h_t = 5$ m, $h_r = 2$ m at T-R separations of (a) 50 m, (b) 200 m and (c) 700 m

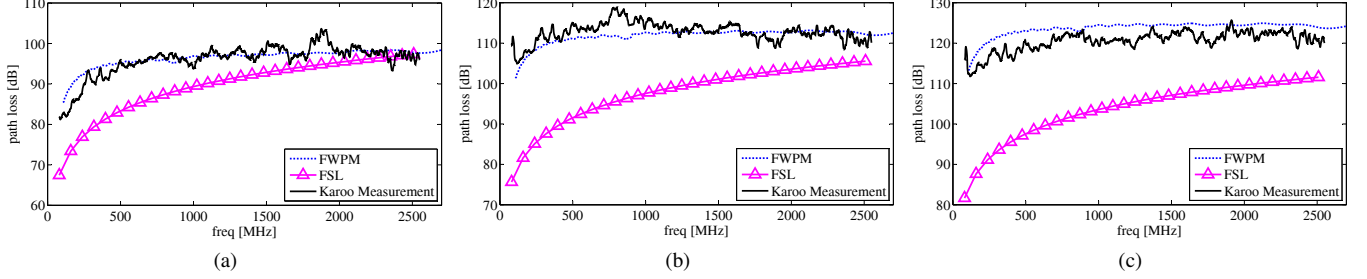


Fig. 7. Measured and predicted path loss in the Karoo: $h_t = 7.5$ m, $h_r = 2$ m at T-R separations of (a) 700 m, (b) 1800 m and (c) 3600 m

TABLE III
STATISTICAL ANALYSIS ON FWPM AND FSL FOR PATH LOSS PREDICTIONS IN THE KAROO

| Case I: $h_t = 5$ m, $h_r = 2$ m | | | | | | | | | | |
|-------------------------------------|------------------------------------|-------|-----------|-------|----------------|-------|----------|-------|--------------------------|-------|
| d_m | Prediction Error, $\bar{\epsilon}$ | | RMSE [dB] | | Relative Error | | Accuracy | | Corr Coefficient, ρ | |
| [m] | FWPM | FSL | FWPM | FSL | FWPM | FSL | FWPM | FSL | FWPM | FSL |
| 50 | 1.31 | 6.13 | 3.33 | 6.97 | 0.034 | 0.080 | 96.60 | 92.01 | 0.956 | 0.979 |
| 200 | -0.05 | 3.18 | 2.11 | 3.88 | 0.018 | 0.043 | 98.19 | 95.75 | 0.951 | 0.944 |
| 700 | -1.30 | 7.73 | 2.25 | 9.25 | 0.016 | 0.081 | 98.38 | 91.86 | 0.783 | 0.702 |
| 1800 | -1.01 | 15.68 | 2.68 | 17.12 | 0.020 | 0.138 | 98.04 | 86.22 | 0.338 | 0.029 |
| 3600 | -4.67 | 17.91 | 5.05 | 18.88 | 0.039 | 0.147 | 96.06 | 85.28 | 0.616 | 0.512 |
| mean 1 | -0.02 | 5.68 | 2.56 | 6.70 | 0.023 | 0.068 | 97.72 | 93.21 | 0.896 | 0.875 |
| mean 2 | -1.15 | 10.13 | 3.08 | 11.22 | 0.025 | 0.098 | 97.45 | 90.23 | 0.729 | 0.633 |
| Case II: $h_t = 7.5$ m, $h_r = 2$ m | | | | | | | | | | |
| 50 | 1.89 | 7.40 | 5.06 | 8.94 | 0.056 | 0.094 | 94.43 | 90.55 | 0.966 | 0.977 |
| 200 | -0.20 | 5.35 | 4.40 | 7.89 | 0.036 | 0.059 | 96.43 | 94.10 | 0.929 | 0.892 |
| 700 | -0.41 | 6.21 | 2.53 | 7.34 | 0.017 | 0.067 | 98.28 | 93.28 | 0.802 | 0.857 |
| 1800 | 0.96 | 14.82 | 2.38 | 16.20 | 0.016 | 0.131 | 98.39 | 86.87 | 0.487 | 0.238 |
| 3600 | -3.12 | 16.56 | 3.47 | 17.26 | 0.026 | 0.138 | 97.38 | 86.21 | 0.792 | 0.819 |
| mean 1 | 0.43 | 6.32 | 3.99 | 8.06 | 0.036 | 0.074 | 96.38 | 92.64 | 0.899 | 0.909 |
| mean 2 | -0.18 | 10.07 | 3.57 | 11.53 | 0.030 | 0.098 | 96.98 | 90.20 | 0.795 | 0.757 |

is presently not problematic since this work does not attempt to determine the value of ϵ_r but focuses on accounting for its effects with respect to obtaining the best predictions. It is probable that the shallow aquifers of the Karoo result in a higher soil moisture content than typical arid regions.

Determining the exact values of complex permittivity is desirable but highly challenging particularly since properties such as compactness and moisture content of the soil change as soon as it has been removed from its locale. Hence, for propagation modelling, finding the best fit using existing data may be the

most practical approach.

Fig 8 shows the magnitude of the Fresnel reflection coefficient as a function of incidence angle ψ (dotted line) as well as the dependence of ψ on distance (solid line) for $h_t = 5$ m. Beyond about 1 km the angle of incidence is negligibly small so that the Fresnel reflection coefficients are independent of complex permittivity and a PEC is approximated. That is, grazing angles yield a reflection coefficient of -1 as predicted by equation (16), indicating a phase shift of 180° which is typically associated with overlap and cancellation of the direct

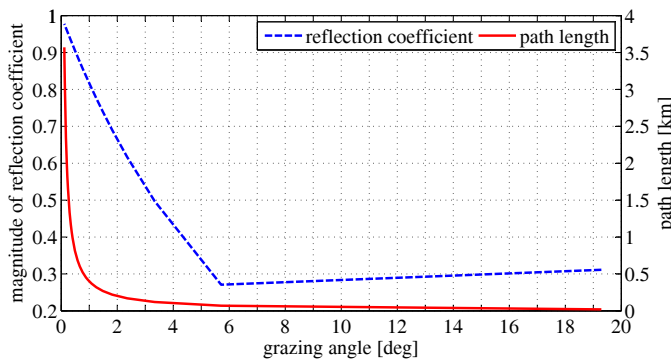


Fig. 8. Fresnel reflection coefficient and the variation of grazing angle with distance

and reflected waves. It is plausible that the relative ‘flattening’ of the path loss curves at 700, 1800 and 3600 m is due to this effect which is most pronounced at the higher frequencies.

V. CONCLUSION

In the Full Wave Propagation Model (FWPM) we have illustrated the implementation of an existing MoM code (FEKO) to predict path loss. The novelty in our work lies in the recreation of a real world measurement scenario wherein antenna characteristics and the influence of the earth are inherently accounted for. Although applied assuming a flat ground, statistical analysis on the FWPM predictions of path loss in the Karoo yielded an impressively low RMSE of < 4 dB. The ability of the FWPM to model propagation over obstacles illustrates the versatility of the method to incorporate more sophisticated scenarios. This has the potential to facilitate easier development of ‘loss’ maps and would be a vital tool for investigating coupling mechanisms, particularly in respect of facilities like MeerKAT.

ACKNOWLEDGEMENT

The financial assistance of the South African SKA Project (SKA SA) towards this research is hereby acknowledged. Opinions expressed and conclusions arrived at are those of the author and are not necessarily to be attributed to the SKA SA. (www.ska.ac.za)

The authors thank EMC consultants MESA Solutions for sharing data and engaging in meaningful discussion. Special thanks to Anneke Bester for technical support during measurements in Stellenbosch.

REFERENCES

- [1] T.S. Rappaport, *Wireless Communications: Principles and Practice*, 2nd ed. New Jersey: Prentice Hall, 2001.
- [2] J. Seybold, *Introduction to RF Propagation*. New Jersey: John Wiley & Sons, Inc., 2005.
- [3] C. Phillips, D. Sicker, and D. Grunwald, “A Survey of Wireless Path Loss Prediction and Coverage Mapping Methods,” *IEEE Communications Surveys & Tutorials*, vol. 15, no. 1, 2013.
- [4] T. K. Sarkar, Z. Ji, K. Kim *et al.*, “A Survey of Various Propagation Models for Mobile Communication,” *IEEE Antennas and Propagation Magazine*, vol. 45, no. 3, 2003.
- [5] V.S. Abhayawardhana, I.J. Wassell *et al.*, “Comparison of Empirical Propagation Path Loss Models for Fixed Wireless Access Systems,” in *Proceedings of the 61st IEEE Vehicular Technology Conference*, 2005.

- [6] H. Harada and R. Prasad, *Simulation and Software Radio for Mobile Communications*. Massachusetts: Artech House, Inc., 2002.
- [7] A.V. Raisanen and A. Lehto, *Radio Engineering for Wireless Communication and Sensor Applications*. Massachusetts: Artech House, Inc., 2003.
- [8] D.B. Davidson, *Computational Electromagnetics for RF and Microwave Engineering*, 2nd ed. Cambridge: Cambridge University Press, 2011.
- [9] J-M. Jin, *Theory and Computation of Electromagnetic Fields*. New Jersey: John Wiley & Sons, Inc, 2010.
- [10] W.C. Gibson, *The Method of Moments in Electromagnetics*. Florida: Chapman & Hall/CRC, 2008.
- [11] E.C. Jordan and K.G. Balmain, *Electromagnetic Waves and Radiating Systems*, 2nd ed. New Jersey: Prentice-Hall Inc., 1968.
- [12] C. A. Balanis, *Advanced Engineering Electromagnetics*, 2nd ed. New York: John Wiley & Sons, Inc., 2012.
- [13] ITU-R, “Rec. ITU-R P.527-3: Electrical Characteristics of the Surface of the Earth,” International Telecommunication Union, Tech. Rep., 1992.
- [14] K.A. Norton, “The Propagation of Radio Waves Over the Surface of the Earth and in the Upper Atmosphere - Part II,” in *Proceedings of the Institute of Radio Engineers*, vol. 25, no. 9, 1937.
- [15] D.J. Angelakos and T.E. Everhart, *Microwave Communications*, ser. Electrical Engineering Series. New York: McGraw-Hill Inc., 1968.
- [16] T.J. Phiri, D.B. Davidson, and P.G. Wiid, “Propagation Modelling for the South African SKA Site,” in *2015 IEEE-APS Topical Conference on Antennas and Propagation in Wireless Communications (APWC)*. IEEE, 2015, pp. 1329–1332.
- [17] A.J. Otto, H.C. Reader, and R.G. Marchand, “Complex Permittivity Measurements of Karoo Soil for the Square Kilometre Array,” in *International Conference on Electromagnetics in Advanced Applications (ICEAA)*, 2011.
- [18] J.T. Hviid, J.B. Andersen, J. Toftgard, and J. Bojer, “Terrain-based propagation model for rural area - an integral equation approach,” *IEEE Transactions on Antennas and Propagation*, vol. 43, no. 1, pp. 41–46, Jan 1995.
- [19] A. Yagbasan, C.A. Tunc *et al.*, “Characteristic basis function method for solving electromagnetic scattering problems over rough terrain profiles,” *IEEE Transactions on Antennas and Propagation*, vol. 58, no. 5, pp. 1579–1589, May 2010.
- [20] C. Brennan and D. Trinh, “Fullwave computation of path loss in urban areas,” in *Antennas and Propagation (EuCAP), 2014 8th European Conference on*, April 2014, pp. 1124–1127.



Temwani J. Phiri Biography text here.



David B. Davidson Biography text here.



P. Gideon Wiid Biography text here.